Energy demand of drive architectures for a wide scope of means of transport: Case-study in Germany

Atiquzzaman Khan Ankur

atiquzzaman.khan.ankur@tecnico.ulisboa.pt

Instituto Superior Técnico, Universidade de Lisboa, Portugal

January 2021

A model is developed to determine the energy demand for passenger and freight transportation within Germany for different transport modes. The modes included are light-duty vehicles (LDVs), heavy-duty vehicles (HDVs), airplanes, trains, ships, and drones. The model further estimates future development until 2050. With standard driving cycles, backward-looking longitudinal vehicle models are used to determine the energy demand for all on-road vehicle modes. For the off-road vehicle modes, real-world energy demand from literature is used to build the model. It is found that various vehicle parameters have different effects on vehicle energy demand, depending on the driving scenario. Public transportation provides the most energy-efficient means of travel in the forms of battery electric and fuel cell buses and coaches, trams, and long-distance electric trains. International shipping is the most energy-efficient means of freight transport. Electrification of drivetrains and the implementation of regenerative braking show a large potential for fuel consumption reduction, especially in urban areas. Occupancy rates for the vehicles play a critical role in determining the energy demand per passenger-kilometer, for passenger modes, and tonne-kilometer, for freight modes.

Keywords: Transport energy demand, Longitudinal vehicle model, Battery electric vehicle, Fuel cell electric vehicle, Vehicle electrification

1. Introduction

A 2019 report by the Intergovernmental Science-Policy Platform on Biodiversity and Ecosystem Services found that around 1 million plant and animal species are under threat of extinction. Some projections show that in the coming decades, the global temperature rise will become the single biggest agent changing ecosystems globally [1]. In 2018 25% of Germany's final energy consumption was in the transportation sector, resulting in 22.7 % of the total emissions of 696 million tonnes of CO2 equivalent (MTCO2e) [2]. Germany has set its target to reduce GHG emissions by 80% to 95%, until 2050, compared to the emissions for the year 1990. Until now, the transport sector has shown the least improvement in emissions reduction [3]. Therefore the German transport sector is facing a massive transformation in an attempt to meet its climate targets. Germany is subsidizing electric vehicle adaption [4] due to its potential for lowering the transport sector's emissions and energy use.

To better understand these transformations and their impacts, a model of the energy demand of all possible transportation modes within Germany must be available. Therefore, this paper aims to develop a model for determining the vehicle-specific energy demand for passenger and freight transportation. The model can distinguish between important possible means of transportation available in Germany and the different drivetrains for each transport mode. Also, it can take into account future developments in energy demand until 2050.

The model is divided into on-road and off-road transport modes. The on-road modes include light-duty vehicles (LDV) and heavy-duty vehicles (HDVs), which are further divided into buses and trucks. The off-road modes include airplanes, drones, trains, and ships. Longitudinal vehicle models are used to determine the energy demand for all on-road vehicle modes. Real-world energy demand from literature is used to build the models for the off-road vehicle modes. In chapter 2, a discussion on the models used to determine transport energy demand in the literature is carried out. Chapter 3 presents a detailed discussion of the model developed for the on-road transport energy demand. Chapter 4 represents the data preparation and validation for the select on-road modes, followed by a discussion of the off-road modes. Chapter 5 discusses the different results obtained from the developed model.

2. Literature Review

In this section, some of the literature models for determining transportation energy consumption are discussed.

2.1. On-road Transport Modes

In the literature, there are many ways of modeling the vehicle energy demand. One of the most widely used is the longitudinal vehicle energy model. In a longitudinal vehicle energy model, the vehicle's lateral and vertical dynamics are neglected, assuming that these do not significantly affect the vehicle energy demand [5]. A backward-looking model is used where the model starts with the traction energy required at the wheels to follow a driving cycle to determine the fuel energy demand for the vehicle [6].

Autonomie and advanced vehicle simulator (ADVISOR) are two of the most widely used vehicle simulators. Autonomie is developed by the Argonne National Laboratory (ANL), while The National Renewable Energy Laboratory developed ADVISOR [7]. Ahmad et al. (2014) carried out modeling and validation of the longitudinal vehicle model. The longitudinal model includes different subsystems for tire, engine, automatic transmission, and braking models. The longitudinal vehicle model is then validated against an experimental vehicle with embedded sensors. The model results are compared with experimental data for sudden braking and throttle imposed motions. It is found that the model results are similar to the experimental results with an acceptable level of error [8].

Edwardes et al. (2014) [9] and Edwardes et al. (2015) [10] use the Virginia Tech Comprehensive Power-Based Fuel Consumption Model (VT-CPFM) to model vehicle energy demand. The VT-CPFM uses a longitudinal vehicle model that considers the effects of aerodynamic drag, rolling resistance, inertial effects, and road gradient. Edwardes et al. (2014) model diesel and hybrid buses. The model is calibrated using publicly available bus parameters. Using the Orange County bus cycle dynamometer test, the model results had an average error of less than 5% [9]. Edwardes et al. (2015) model diesel buses [10]. Park et al. (2013) validate the VT-CPFM with real-world fuel consumption measurements. The model is calibrated using the United States Environmental Protection Agency (US EPA) city and highway fuel economy ratings [11]. Gao et al. (2007) highlight the need for modeling electric vehicles and HEV [6]. Grube et al. (2018) analyzed the impact of driving cycles and auxiliary power in passenger cars' fuel energy demand. The analysis includes ICEV, HEV, BEV, and FCEV and focuses on reducing fuel consumption using electric power [12].

Abousleiman et al. (2015) [13], Fiori et al. (2016) [7], and Luin et al. (2019) [14] analyze the energy demand for electric vehicles (EV). Abousleiman et al. (2015) use a longitudinal vehicle model and compare the results obtained with data from driving the modeled vehicle in real-world driving conditions. The impacts of auxiliary loads are also considered in the form of the vehicle's heating, ventilation, and air conditioning (HVAC) power demand and power needed for battery conditioning and other drivetrain-related power [13]. Fiori et al. (2016) develop a model to estimate the instantaneous power requirements for electric vehicles using second-by-second vehicle speed, acceleration, and road grade data as input to the model. The model used is a quasi-steady backward-looking longitudinal vehicle model due to its fast simulation times [7]. Luin et al. (2019) develop a model to simulate the energy consumption of EVs. A longitudinal vehicle energy model is used to determine vehicle energy demand [14].

Abousleiman et al. (2015) use a constant efficiency value to model the regenerative braking power [13]. Fiori et al. (2016) also calculate the instantaneous energy regeneration from braking. It shows that EVs can regenerate higher energy in urban driving conditions than highway driving conditions [7]. Fiori et al. (2016) consider the effects of auxiliary systems like air conditioning and heating systems. It demonstrates that the use of HVAC systems can reduce the EV range [7]. Abousleiman et al. (2015) model the HVAC power requirement, using a function that varies with the ambient temperature. The power demand for cabin HVAC is negligible for ambient temperatures between approximately 14 and 27 °C, according to this model [13]. Grube et al. (2018) use a simplified thermal model to determine the vehicle cabin's HVAC energy requirements [12].

2.2. Off-road Transport Modes

Between 1990 and 2018, international aviation had the highest relative increase, 124.6%, compared to other transportation modes, in energy consumption within the EU [15]. In Germany, aviation is responsible for 15% of all transport-related CO2 emissions for 2014, the second-highest after road vehicles [16]. Therefore, airplane fuel energy demand must be taken into account in any transport sector's holistic model.

Burzlaff (2017) develops a model to determine the fuel consumption of airplanes. The model can evaluate type-specific fuel consumption using publicly available airplane information [17]. Park et al. (2014) model the airplane fuel burn for different aircraft models globally. The paper finds that flight lengths between 1500 and 2000 nautical miles are the most fuel-efficient flights [18]. Peeters et al. (2005) assess the change in commercial airplanes' fuel efficiency from the 1930s to the 2000s [19]. Kharina et al. (2015) discuss the fuel efficiency trends for airplanes between 1960 and 2014 [20]. Xu (2017) models the energy demand of different sized freight drones [21]. Bauhaus Luftfahrt reports the energy demand for passenger drones [22].

The energy demand for railways needs to be further studied in order to save energy due to environmental concerns and high energy costs [23]. Salvador et al. (2018) develop a dynamic model to estimate the energy consumption of diesel trains. Comparison of the model results against real operational data shows an error rate of below 9% [24]. Wang et al. (2017) build a model to determine the energy consumption of electric trains. The model is calibrated using data from Oregon, United States, and validated using data from the National Transit Database. The model results are sufficiently accurate. The model shows that the use of regenerative braking can save around 20% of energy consumption. The model can take into account the effects of train models, route, and operational parameters [25].

The shipping industry is responsible for transporting the vast majority of global trade [26]. Jeon et al. (2018) predict ships' fuel consumption by using artificial neural networks to analyze ships' big data. The paper reports this method to be more accurate and efficient than polynomial regression and support vector machine [27]. Yang et al. (2019) model the fuel consumption for ships using a genetic algorithm-based grey-box model. This model's advantage over other grey-box models is that it can better account for oblique weather directions [28].

One of the main differences between the model being developed in this paper and the ones mentioned above is the number of different modes of transport. Germany's different transport modes must be modeled to get an overview of the German transport network's energy demand. The models mentioned above only simulate specific transport modes. The model developed in this paper considers LDVs, HDVs (buses and trucks), aviation modes (including conventional fixed-wing planes and electric drones), trains, and ships. These modes are further subdivided into passenger and freight modes. Another difference with the published literature is that the proposed model can analyze the effects of different occupancy rates, i.e., the energy requirements to transport each passenger, or a tonne of cargo, can then be analyzed. The model also considers the effects of driving conditions like ambient temperatures and driving scenarios for on-road transport modes.

3. Methodology

This section discusses the physics behind the implemented model used to determine the on-road vehicle's mechanical energy demand, followed by a discussion of the effects of regenerative braking systems and the model used to determine the final fuel energy demand of the vehicle. The physics behind the simulation being used for on-road vehicles are extensively discussed, as it will also be the most detailed part of the final model.

The drivetrain of a vehicle converts the stored energy in the fuel to the vehicle's mechanical energy, used to overcome the driving resistances. There are three main types of driving resistances [29]

1. Aerodynamic friction
2. Rolling friction
3. Energy dissipated in the brakes

These resistances can be represented in a differential form as;

$$m_{e,v}\frac{d}{dt}v(t) = F_{trac}(t) - \left(F_a(t) + F_r(t) + F_g(t) + F_d(t)\right) \quad (1)$$

Where

F_a = aerodynamic friction
F_r = rolling friction
F_g = gravitational force for non-horizontal roads
F_d = disturbance forces
F_{trac} = traction force at the wheel
$m_{e,v}$ = equivalent mass of the vehicle and occupants
v = speed of the vehicle

This model is referred to as the longitudinal vehicle model because it only considers the vehicle dynamics in the vehicle's longitudinal axis. It does not consider the lateral forces on the vehicle.

Equation 2 gives a general overview of energy pathways in a vehicle. F_d represents any external forces acting on the vehicle. F_{trac} is the force being generated at the wheel to propel the vehicle. The effects of vertical lift force are neglected.

Aerodynamic friction, rolling resistance, gravitational forces, and the vehicle's equivalent mass are calculated [29].

$$F_a(v) = \frac{1}{2}\cdot\rho_a\cdot A_f\cdot c_a\cdot v^2 \quad (2)$$

$$F_r = c_r\cdot m_v\cdot g \quad (3)$$

$$F_g(\alpha) = m_v\cdot g\cdot \alpha \quad (4)$$

where v is the vehicle speed, ρ_a is the density of the air, A_f is the frontal area, c_a is the aerodynamic drag coefficient, m_v is the vehicle's mass along with passengers and cargo, g is the gravitational acceleration, and α is the gradient of the road.

The rolling resistance c_r is assumed to be dependent on the vehicles' speed alone [30].

$$c_r = 0.0088 + 0.0017 \cdot \frac{v}{100} + 0.00028 \cdot \left(\frac{v}{100}\right)^4 \quad (5)$$

m_{ev} represents the vehicle's mass, and occupants, along with the rotational inertia of all the rotating masses [29]. An estimate of the vehicle equivalent mass $m_{e,v}$ can be found by multiplying the vehicle mass m_v with the rotational inertia factor δ and adding the occupant mass m_{occ}.

$$m_{e,v} = m_v \cdot \delta + m_{occ} \quad (6)$$

For this model, an average rotational inertia factor of 1.02 is assumed for all LDV and HDV vehicles [31]. It must be taken into account that this factor must be multiplied by the vehicle mass only, not including the cargo and passenger mass (occupant mass).

Multiplying the equivalent vehicle mass with the vehicle acceleration gives the force required for the vehicle's acceleration, also known as the motive force [31].

Traction force is the force that the wheel has to exert on the road to propel the vehicle against the resisting forces. No-slip condition is assumed between the tire and the road. Thus the wheel torque is wholly transferred to the road [32].

Therefore, to find the traction force, the driving mode must first be determined. There are three possible driving conditions [29].

1. Traction mode: the engine is doing work in moving the vehicle,
2. Braking mode: brakes are dissipating energy to slow down the vehicle
3. Coasting mode: the vehicle is moving under its own stored mechanical energy

The vehicle's coasting velocity is calculated using equation 7, assuming no disturbance force and setting the traction force to zero. It results in the following equation for the coasting velocity [29]

$$\frac{d}{dt}v_c(t) = \frac{-1}{2 \cdot m_{e,v}} \cdot \rho_a \cdot A_f \cdot c_a \cdot v_c^2(t) - g \cdot c_r - g \cdot \alpha \quad (7)$$

The above equation can be easily solved using a numerical method. In this case, the forward Euler method is used [33]. By comparing the result with the actual vehicle velocity $v(t)$ from the driving cycle, the driving mode can be determined [29].

A vehicle is in traction mode if $v(t) > v_c(t)$, in braking mode if $v_c(t) > v(t)$, and in coasting mode if $v_c(t) = v(t)$, for a finite time interval. According to this model, the vehicle speed and the road gradient must be predetermined to find the wheel's traction force. The predetermined speed is provided by the standard driving cycles.

The vehicle's mechanical energy demand is the energy that the vehicle needs to follow the chosen driving cycle. The key parameter used in this calculation is the mean tractive force, $\bar{F}_{trac}$. The mean tractive force is defined as

$$\bar{F}_{trac} = \frac{1}{x_{tot}} \cdot \int_{t \in trac} F(t) \cdot v(t) dt \quad (8)$$

where $trac$ is the time intervals where $F_{trac} > 0$, in other words, those parts of the cycle when the vehicle is in traction mode, and x_{tot} is the total distance traveled during the cycle. The parts of the driving cycle when the vehicle is in braking mode ($F_t < 0$) or coasting mode ($F_{trac} = 0$), the vehicle does not require any mechanical energy from the drivetrain. The energy necessary for aerodynamic and rolling resistances is covered by the decrease of the vehicle's mechanical energy.

The 0% and 100% brake energy recuperation scenarios are next considered. If the vehicle is not fitted with a braking energy recuperation device, equation 9 is applicable. Thus, there are four significant contributions to the traction force

$$\bar{F}_{trac} = \bar{F}_{trac,a} + \bar{F}_{trac,r} + \bar{F}_{trac,m} + \bar{F}_{trac,g} \quad (9)$$

For a vehicle with perfect recuperation efficiency, there are only three significant contributions to the traction force

$$\bar{F}_{trac} = \bar{F}_{trac,a} + \bar{F}_{trac,r} + \bar{F}_{trac,g} \quad (10)$$

This is because any energy spent accelerating the vehicle is wholly recuperated during the braking phases by the recuperation device. Therefore, the energy consumed in the acceleration phase is ignored. The summations must be carried out over the entire driving cycle and not just the traction regions. As 100% efficiency is not feasible in a real-world scenario, the model will interpolate the actual energy demand based on the "No Recuperation" and "Perfect Recuperation" energy demands.

$$\bar{F}_{trac}(\eta_{rec} = rec) = \bar{F}_{trac}(\eta_{rec} = 100\%) + (1 - rec) \cdot (\bar{F}_{trac}(\eta_{rec} = 0\%) - \bar{F}_{trac}(\eta_{rec} = 100\%)) \quad (11)$$

where η_{rec} is the recuperation efficiency, rec is the actual recuperation efficiency of the vehicle as a fraction, $\eta_{rec} = 0\%$ is the "No Recuperation" scenario, $\eta_{rec} = 100\%$ is the "Perfect Recuperation" scenario, and $\eta_{rec} = rec$ is the scenario for the given recuperation efficiency.

Finally, the mechanical energy demand E_{mech} for the vehicle is calculated using the mean tractive force. The mean tractive force is equal to the average energy consumed per distance traveled. When the mechanical energy demand is expressed in units of MJ/100km, the relationship between the quantities is

$$E_{mech} = \frac{\bar{F}_{trac}}{10} \quad (12)$$

After calculating the vehicle's mechanical energy demand, the next major energy demand must be taken into account. These include the powers needed for the vehicle's HVAC system and other essential parts of the vehicle. These systems are combined into one in this model and is referred to as auxiliary power P_{aux} demand. The auxiliary power demand is used as an input to the model. The auxiliary energy E_{aux} demand is then calculated as follows

$$E_{aux} = \sum_{i=1}^{n} P_{aux} \cdot h \quad (13)$$

Therefore, the energy provided by the drivetrain is the summation of the E_{mech} and E_{aux} demand of the vehicle. The drivetrain efficiency is then taken into account to find the final fuel energy demand for the vehicle. In the cases where the vehicle has two different energy storages or motors, the mechanical and auxiliary energy demands are shared based on the driving share ratios. The final fuel energy demands are then calculated separately for individual storage and motor. Finally, the overall fuel energy demand is calculated by summing the individual fuel energy demands.

4. Data Preparation and Validation

4.1. On-road Transport Modes

4.1.1. Standard driving cycles

Standard driving cycles are speed versus time profiles that try to mimic real-world vehicle operation [34]. Worldwide Harmonized Light Vehicles Test Cycle (WLTC) is developed to give better laboratory estimates for real-world vehicle emissions and fuel consumption for LDVs [35].

The WLTC class 3b is divided into four distinct driving scenarios; Low, Medium, High, and Extra-High speed regions, representing Urban, Suburban, Rural, and Highway scenarios, respectively. Figure 1 shows the driving cycle [35].

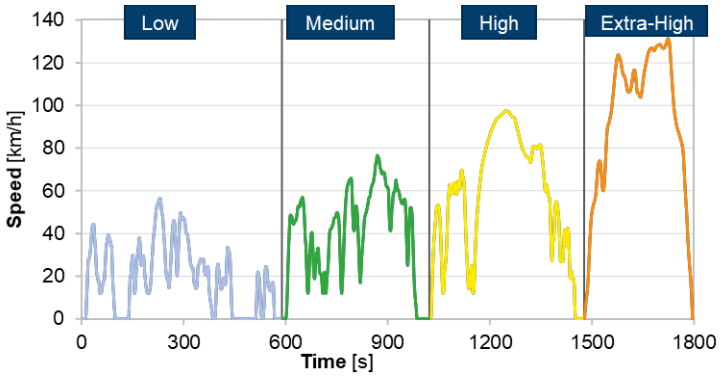

Figure 1: WLTC class 3b with different driving scenarios (Adapted from [35]*)*

As can be seen from Figure 1, the driving cycle has distinct driving characteristics for the four different driving scenarios. WLTC class 3b is used by default to model the energy demand of all LDVs. Other driving cycles are also available within the model to simulate different driving conditions.

4.1.2. Validation

Here the model results for ICEV, FCEV, and BEV drivetrains of chosen modes are compared with data from literature and real vehicles to confirm the model's validity.

Figure 2 shows the ICEV-g, FCEV, and BEV energy demands of medium cars predicted by the model compared to energy demand data reported for various vehicle manufacturers.

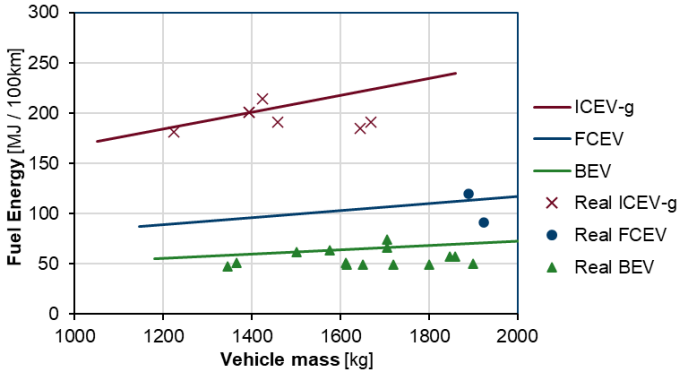

Figure 2: Comparison of real and model energy demand for medium cars for different vehicle mass. The solid lines represent model results.

As can be seen from Figure 2, the model results agree well with reported values for real vehicles in the market.

The results for medium buses, Figure 3, and large trucks, Figure 4, are validated using data reported for current vehicles in the literature.

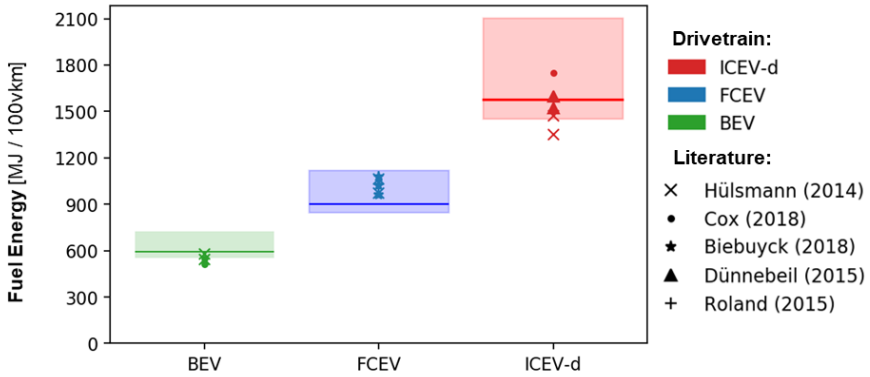

Figure 3: Model vs. Literature energy demand for medium buses [36], [37], [38]*. Solid lines represent the fuel energy demand for the average occupancy rate. The shaded area represents the energy demand for varying occupancy rates between 0% and 100%, according to the model.*

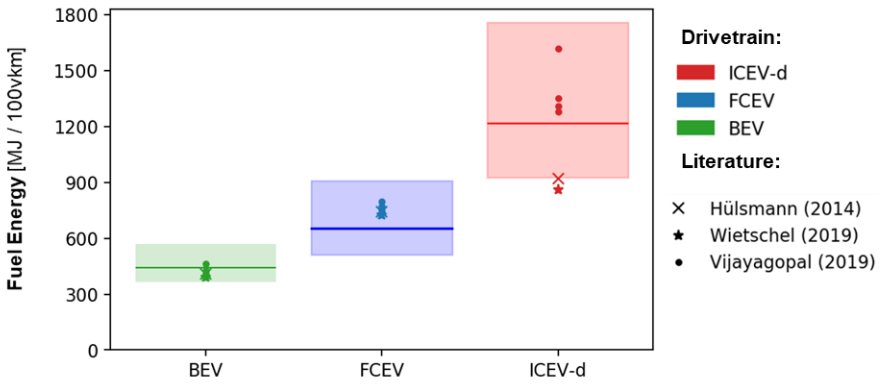

Figure 4: Model vs. Literature energy demand for large trucks [36], [39], [40]*. Solid lines represent the fuel energy demand for the average occupancy rate. The shaded area represents the energy demand for varying occupancy rates between 0% and 100%, according to the model.*

In Figure 3 and Figure 4, the range of values shown by the shaded region represents the energy demand for different occupancy rates. The solid line represents the energy demand for the average occupancy rate in Germany. As can be noted, the results from the model match well with the literature values. Therefore, it can be concluded that the model results are valid.

4.2. Off-road Transport Modes

4.2.1. Airplanes

For airplanes, flight distance has a significant impact on fuel energy consumption. A flight distance of 2700 to 3700 km is the most fuel-efficient flight distance for the average passenger airline [17]. Due to the complex physics of aircraft flight, a different approach is considered for the aviation fuel demand model.

Firstly the German aviation industry must be better understood. Lufthansa Group has the largest market share, at 87.1 % as of 2018 [41], of the German aviation industry, second largest in Europe [42]. In addition to the aircraft in the Lufthansa Group's fleet, other widely-used models in the industry are also considered to increase the fuel demand results' robustness.

The Aviation Emissions Calculator (AEC) accompanying the EMEP/EEA air pollutant emission inventory guidebook is then used to find out the fuel burned by the selected aircraft models for different flight distances [43]. Figure 5 shows the total seating and cargo capacity as a function of the flight distance used in the model.

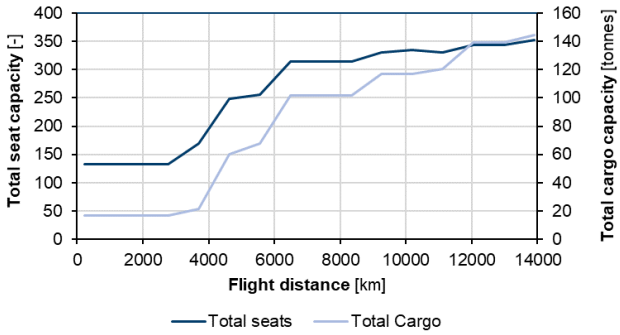

Figure 5: Seating and Cargo capacity as a function of flight distance.

For each discrete flight distance, multiple possible aircraft models are chosen. The future improvement in energy demand per decade is approximately 10% [20].

4.2.2. Drones

Jia Xu (2017) models the energy demand of different sized freight drones. Figure 6 below shows the energy demand for the delivery as a function of the flight distance [21].

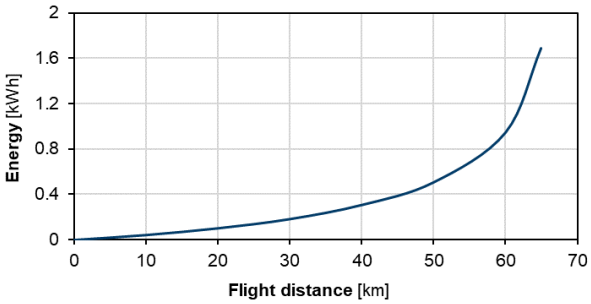

Figure 6: Freight drones energy demand for Amazon Prime Drone with a maximum capacity of 2.3kg [21]

Bauhaus Luftfahrt reports the energy demand for the two major passenger drone configurations; multicopter and lift+cruise configuration. The results show that multicopter drones require less energy, although their flight range is limited compared to lift+cruise drones. Figure 7 shows the energy demand per passenger-kilometer for different flight distances for drones with four passengers' maximum capacity [22].

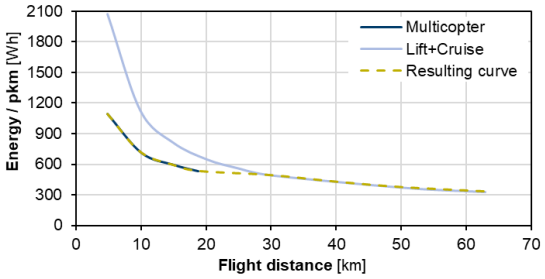

Figure 7: Passenger drones energy demand for drones with a maximum capacity of four passengers [22]

Figure 7 also shows the resulting curve used to model the energy demand for passenger drones.

4.2.3. Trains

Trains are an important mode of transport. Rail transportation was responsible for 4.5% of the total transport sector carbon emissions for the year 2014 in Germany [16]. The railway model is based on literature data and considers four different modes; trams, short and long-distance trains, and freight trains.

For the trams, Kuminek (2013) reports the energy consumption values for electric catenary trams [44]. Energy demands for electric and diesel short-distance trains and freight trains can be found from the Global Emissions Model for integrated Systems (GEMIS) database [45]. The data for long-distance trains is taken from Deutsche Bahn's Integrated Report [46]. The FCEV freight train data is based on Bründlinger et al. (2018) [47].

4.2.4. Ships

The importance of ships in global freight transport can not be understated. Shipping accounts for about 75% of global freight transportation, and it does so, being the most energy-efficient means of carrying cargo [48].

Similar to trains and aviation models, the shipping model is based on literature data. The energy demand for international shipping is taken from IEA [48], while that for national shipping (inland waterway transport) is based on Bründlinger et al. (2018) [47].

5. Results and Discussions

The results obtained from the developed model are discussed in this section. Firstly, the effects of varying vehicle parameters are analyzed for different driving conditions in section. A modal analysis is carried out for both passenger and freight transport modes. The energy consumption of different drivetrains for a medium car is next analyzed. The effects of electrification on the energy demand of a vehicle are then discussed. Next, the effects of the driving environment on energy demand for trucks and buses are assessed. The section concludes with a comparison of the results from the model with other studies.

5.1. Parameter variation

In this section, the effects of changing the vehicle's mass, aerodynamic properties, and rolling resistance on a battery-electric medium car's fuel energy demand are analyzed. The effects are analyzed for urban and highway driving conditions, Figure 8.

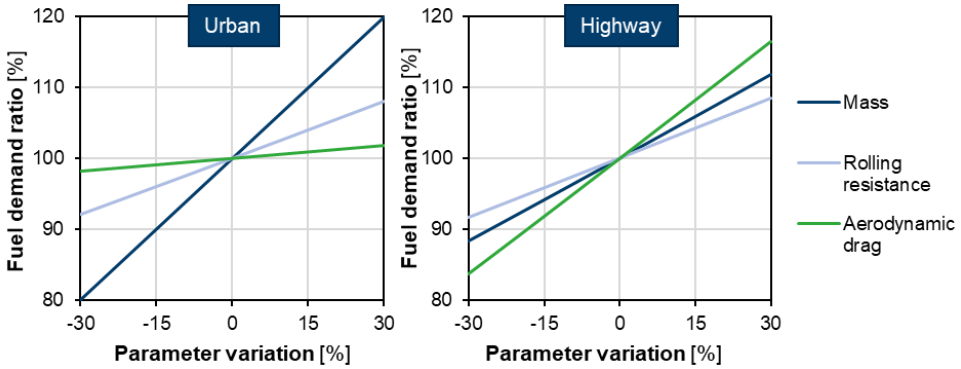

Figure 8: Effects of parameter variation on fuel demand for BEV over urban (left) and highway (right) driving scenarios

Figure 8 shows that reducing vehicle mass has the highest effect on urban driving conditions due to the stop-and-go driving prevalent in urban driving. 10% reduction in vehicle mass resulted in a 6.7% lower fuel energy demand. If the vehicle did not have regenerative braking, the effects would be more pronounced. Changing the aerodynamic drag has the least impact on the final energy demand due to the low average speed in urban conditions. The aerodynamic drag force is proportional to the vehicle velocity square.

Figure 8 shows that changing the aerodynamic drag has the highest impact on the energy demand for highway driving conditions due to the higher speeds in highway driving, which results in a higher proportion of the total energy demand used to overcome the aerodynamic drag. A 10% improvement in vehicle aerodynamics reduced energy consumption by 5.5%. Rolling resistance variation has the least impact on vehicle energy demand for highway driving.

5.2. Modal Analysis

This section discusses the fuel energy demand for conventional, hydrogen, and electric drivetrains of the different passenger modes. Figure 9 shows the fuel demand for select short-distance passenger transport modes, in terms of energy per 100 passenger-kilometer (pkm), for varying occupancy rates, while Figure 10 shows the same data but without the drones. The default occupancy rates for 2020 are highlighted for each drivetrain.

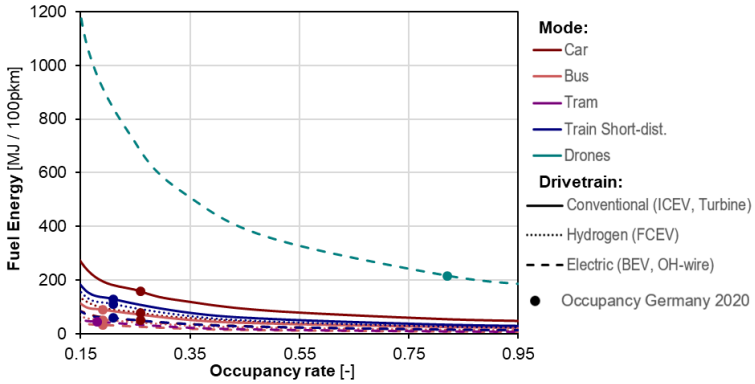

Figure 9: Fuel energy demand vs. occupancy rate for select short-distance passenger modes

As shown in Figure 9, drones have the highest energy consumption for short-distance passenger transport, 217 MJ/100pkm for the average occupancy rate.

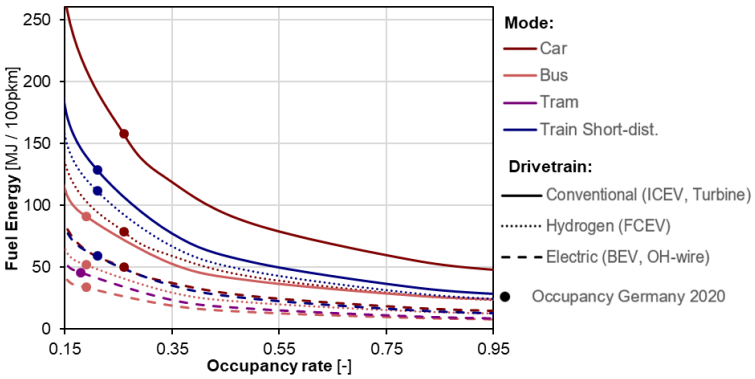

Figure 10: Fuel energy demand vs. occupancy rate for short-distance passenger modes, without drones

Figure 10 shows that, after drones, ICEV-g medium cars (158 MJ/100pkm) have the highest energy consumption for all occupancies. In contrast, battery-electric cars and buses, fuel cell buses, and trams have some of the lowest, at 50, 34, 52, and 46 MJ/100pkm, respectively.

Overall, Figure 9 and Figure 10 clearly show the effects of occupancy rates on the fuel demand per passenger-kilometer. The exponential rise in energy demand for low occupancy rates shows the importance of high occupancy rates in reducing the overall transport sector energy demand while still maintaining passenger capacity.

Figure 11 shows the fuel demand for select long-distance passenger transport modes, in terms of energy per 100 passenger-kilometer (pkm), for varying occupancy rates, while Figure 12 shows the same data but without the airplane modes. The default occupancy rates for 2020 are highlighted for each drivetrain.

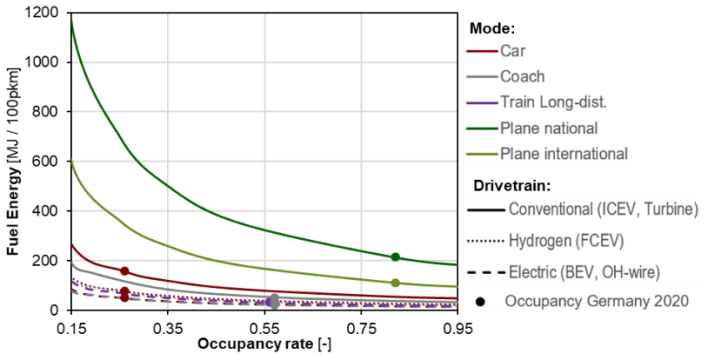

Figure 11: Fuel energy demand vs. occupancy rate for select long-distance passenger modes

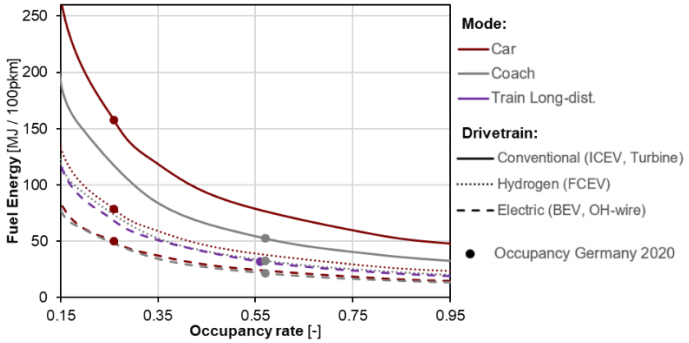

Figure 12: Fuel energy demand vs. occupancy rate for long-distance passenger modes, without airplanes

Figure 11 shows that airplanes have the highest energy demand for all occupancy rates, with national flights coming on top (215 MJ/100pkm).

Figure 12 shows that, after airplanes, ICEV-g medium cars (158 MJ/100pkm) have the highest energy consumption for all occupancies, while BEV and FCEV coaches and long-distance trains have the least, at 21, 33, and 32 MJ/100pkm, respectively.

5.3. Drivetrain Analysis

In this section, the energy demands for the different drivetrains of medium cars are discussed. The energy demand for the different drivetrains until 2050 is shown in Figure 13, in terms of energy per 100 vehicle-kilometer (vkm).

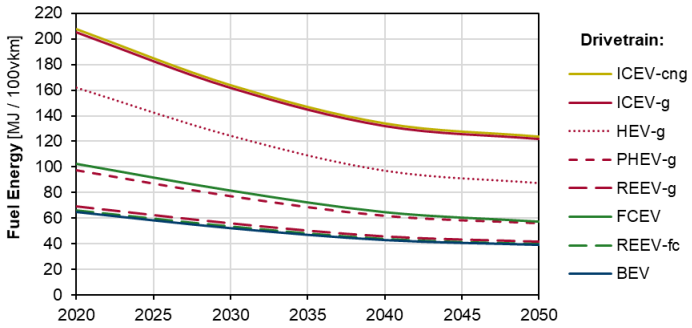

Figure 13: Energy demand for different drivetrain medium cars until 2050

Figure 13 shows that ICEVs have the worst energy demand amongst all the different drivetrains. HEV-g shows lower energy consumption values due to better drivetrain efficiencies and the use of regenerative braking. PHEV-g and REEV-g have even lower energy consumption values due to the all-electric driving option. BEV has the best energy consumption values.

Furthermore, HEV-g shows the most significant relative improvement until 2050 of 45.7%, while BEV shows the least, 39.6%. In terms of energy demand, ICEV-cng and ICEV-g both reduce their energy demand by roughly 80 MJ/100vkm to reach around 120 MJ/100vkm by 2050.

5.4. Electric share

In this section, the change in fuel energy demand with increased drivetrain electrification is analyzed. An HEV-g medium car is considered for a vehicle with 0% electric drive share, while a BEV represents a vehicle with a 100% electric share. A PHEV-g car is used to model electric drive shares in between. Figure 14 shows the result of this analysis.

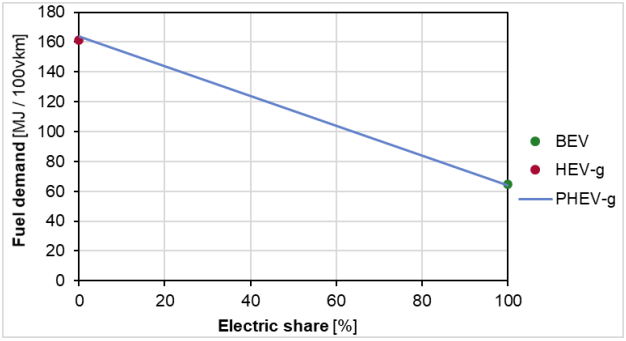

Figure 14: Fuel energy demand vs. electric share for medium car

Figure 14 shows how fuel energy demand drastically decreases with the increase in electric share. A drivetrain with a 100% electric share has almost 60% lower fuel demand than a drivetrain with a 0% electric share. It is assumed that PHEV has the same configuration (battery capacity) and, therefore, the same vehicle mass. Only user behavior leads to different electric shares.

5.5. Effects of Driving Environment

5.5.1. Trucks for different purposes

The energy demands for trucks used for different functions are analyzed first. A small truck used for urban cargo delivery is analyzed using the urban and rural parts of the World Harmonized Vehicle Cycle (WHVC). A large truck used for urban waste collection is analyzed using the Neighborhood Refuse Truck Cycle. Finally, a semi-truck used for long-haul freight transportation is evaluated using the highway segment of the WHVC. Default occupancy rates are assumed for all modes. Figure 15 shows the results obtained from this analysis.

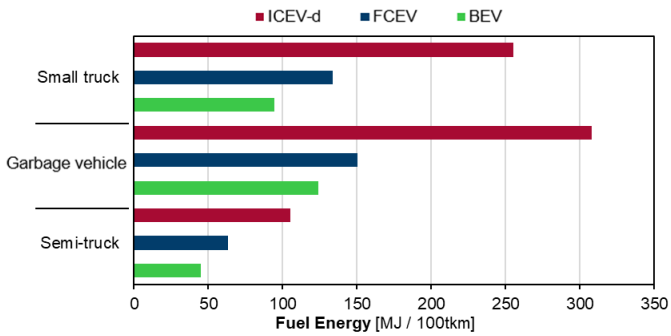

Figure 15: Fuel energy demand for a small truck (urban cargo), garbage vehicle, and semi-truck (long-haul)

Figure 15 shows that urban waste collection is the most energy-intensive while long-haul freight transport is the least energy-intensive for all drivetrains. Urban cargo and waste collection benefit the most from drivetrain electrification, with roughly a 60% drop in fuel energy demands. This is

due to the prevalence of stop-and-go driving conditions for these vehicles. Long-haul cargo is the least energy-intensive due to their higher occupancy rates and the lack of stops, significantly impacting trucks' energy demand due to their massive masses.

5.5.2. Effects of ambient temperature for buses

The impact of the ambient temperature variation on the fuel energy demand for a medium bus is analyzed next, over a temperature range of -10 to 25 °C, Figure 16.

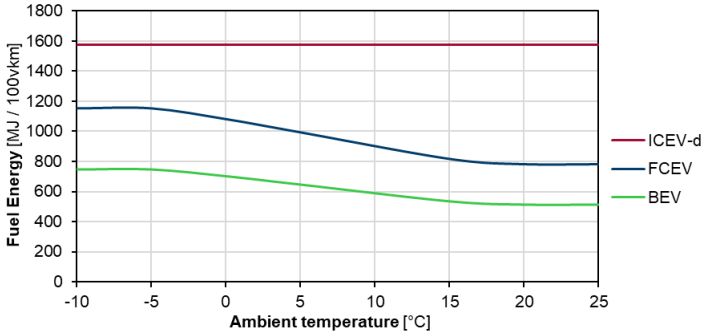

Figure 16: Fuel energy demand for medium buses for varying ambient temperature.

Figure 16 shows that the energy demand for ICEV-d does not change with temperature variation, assuming the engine's waste heat meets the thermal energy requirements. For FCEV and BEV, the energy demand depends on the ambient temperatures between approximately -5 and 17°C. It is assumed that the vehicle only needs to use ventilation for higher temperatures, and for lower temperatures, it is assumed that the vehicle's heating capacity is reached. Going from a temperature of 20 °C to -5 °C, the vehicle's fuel energy demand increases by almost 50%.

6. Conclusion

The German transport sector is in the midst of a massive transformation in an attempt to meet its climate targets. In this regard, it is expected that there will be profound modal shifts in the transport sector. This paper aimed to build an energy model for the major modes of transport in Germany. Furthermore, future efficiency improvements were also considered for the various modes. The results were found to be valid by comparison with real vehicles and data from the literature.

Driving conditions were the most important criterion when comparing the vehicle energy demand between drivetrains. On the other hand, occupancy rates were the most critical indicator when comparing energy demand between the different modes.

For both short- and long-distance passenger transport, public transportation was often the most energy-efficient means. For short-distance journeys, battery-electric buses (33.9 MJ/100pkm) and trams (45.8 MJ/100pkm), and for long-distance journeys, battery-electric coaches (21.3 MJ/100pkm) and electric trains (31.8 MJ/100pkm) represented the best energy efficiencies. The aviation modes considered in this model generally had the highest energy consumption, between 110 and 217 MJ/100pkm.

For freight transportation, international shipping (9.9 MJ/100tkm) was the most energy-efficient while national flights the least (1726 MJ/100tkm). For national freight transport, electric trains (35.2 MJ/100tkm), as well as battery-electric (45.1 MJ/100tkm) and fuel-cell (64.2 MJ/100tkm) semi-trucks were some of the best modes.

In future transport scenarios, the first aim should be to increase occupancy rates. It will be challenging to implement, but it is a free upgrade, as no additional investment in technology is required to decrease the energy intensity of transport. Furthermore, increased electrification of drivetrains will reduce the final energy demand for the transport sector.

7. Bibliography

[1] IPBES, "SUMMARY FOR POLICYMAKERS OF THE IPBES GLOBAL ASSESSMENT REPORT ON BIODIVERSITY AND ECOSYSTEM SERVICES," 2019. [Online]. Available: https://ipbes.net/system/tdf/ipbes_global_assessment_report_summary_for_policymakers.pdf?file=1&type=node&id=35329.

[2] "Data & Statistics - IEA," *The Federal Minister for the Environment, Nature Conservation, and Nuclear Safety*, 2019. https://www.iea.org/data-and-statistics?country=WORLD&fuel=CO2 emissions&indicator=CO2 emissions by sector (accessed Jul. 04, 2020).

[3] "Climate Action Plan 2050 – Germany's long-term emission development strategy | BMU," *The Federal Minister for the Environment, Nature Conservation, and Nuclear Safety*. https://www.bmu.de/en/topics/climate-energy/climate/national-climate-policy/greenhouse-gas-neutral-germany-2050/ (accessed Jul. 05, 2020).

[4] S. Amelang, "Germany commits additional €3 bln to ease green mobility transition in car industry," *Clean Energy Wire*, 2020. https://www.cleanenergywire.org/news/germany-commits-additional-eu3-bln-ease-green-mobility-transition-car-industry (accessed Dec. 14, 2020).

[5] P. Jardin, A. Esser, S. Givone, T. Eichenlaub, J.-E. Schleiffer, and S. Rinderknecht, "The Sensitivity in Consumption of Different Vehicle Drivetrain Concepts Under Varying Operating Conditions: A Simulative Data Driven Approach," *Vehicles*, vol. 1, no. 1, pp. 69–87, 2019, doi: 10.3390/vehicles1010005.

[6] D. W. Gao, C. Mi, and A. Emadi, "Modeling and Simulation of Electric and Hybrid Vehicles," *Proc. IEEE*, vol. 95, no. 4, pp. 729–745, Apr. 2007, doi: 10.1109/JPROC.2006.890127.

[7] C. Fiori, K. Ahn, and H. A. Rakha, "Power-based electric vehicle energy consumption model: Model development and validation," *Appl. Energy*, vol. 168, pp. 257–268, 2016, doi: 10.1016/j.apenergy.2016.01.097.

[8] F. Ahmad, S. A. Mazlan, H. Zamzuri, H. Jamaluddin, K. Hudha, and M. Short, "MODELLING AND VALIDATION OF THE VEHICLE LONGITUDINAL MODEL," *Int. J. Automot. Mech. Eng.*, vol. 10, no. 12, pp. 2042–2056, Dec. 2014, doi: 10.15282/ijame.10.2014.21.0172.

[9] W. Edwardes and H. Rakha, "Virginia tech comprehensive power-based fuel consumption model," *Transp. Res. Rec.*, vol. 2428, no. 2428, pp. 1–9, 2014, doi: 10.3141/2428-01.

[10] W. Edwardes and H. Rakha, "Modeling diesel and hybrid bus fuel consumption with Virginia Tech comprehensive power-based fuel consumption model: Model enhancements and calibration issues," *Transp. Res. Rec.*, vol. 2533, no. 2533, pp. 100–108, 2015, doi: 10.3141/2533-11.

[11] S. Park, H. Rakha, K. Ahn, and K. Moran, "Virginia Tech Comprehensive Power-based Fuel Consumption Model (VT-CPFM): Model Validation and Calibration Considerations," *Int. J. Transp. Sci. Technol.*, vol. 2, no. 4, pp. 317–336, 2013, doi: 10.1260/2046-0430.2.4.317.

[12] T. Grube and D. Stolten, "The impact of drive cycles and auxiliary power on passenger car fuel economy," *Energies*, vol. 11, no. 4, 2018, doi: 10.3390/en11041010.

[13] R. Abousleiman and O. Rawashdeh, “Energy consumption model of an electric vehicle,” *2015 IEEE Transp. Electrif. Conf. Expo, ITEC 2015*, no. 1, 2015, doi: 10.1109/ITEC.2015.7165773.

[14] B. Luin, S. Petelin, and F. Al-Mansour, “Microsimulation of electric vehicle energy consumption,” *Energy*, vol. 174, pp. 24–32, 2019, doi: 10.1016/j.energy.2019.02.034.

[15] “Energy statistics-an overview Statistics Explained.” Accessed: Oct. 15, 2020. [Online]. Available: https://ec.europa.eu/eurostat/statisticsexplained/.

[16] “Energiewende Outlook: Transportation sector.” Accessed: Sep. 10, 2020. [Online]. Available: www.pwc.de/energy-transition.

[17] M. Burzlaff, “Aircraft Fuel Consumption - Estimation and Visualization,” *Fuel Consum.*, 2017, doi: 10.15488/2553.

[18] Y. Park and M. E. O’Kelly, “Fuel burn rates of commercial passenger aircraft: Variations by seat configuration and stage distance,” *J. Transp. Geogr.*, vol. 41, pp. 137–147, 2014, doi: 10.1016/j.jtrangeo.2014.08.017.

[19] P. Peeters, J. Middel, and A. Hoolhorts, “Fuel efficiency of commercial aircraft: An overview of historical and future trends,” Amsterdam, 2005. doi: http://www.transportenvironment.org/Publications/prep_hand_out/lid/398.

[20] A. Kharina and D. Rutherford, “Fuel efficiency trends for new commercial jet aircraft : 1960 to 2014,” Washington, 2015. [Online]. Available: https://theicct.org/publications/fuel-efficiency-trends-new-commercial-jet-aircraft-1960-2014.

[21] J. Xu, “Design Perspectives on Delivery Drones,” RAND Corporation, 2017. doi: 10.7249/RR1718.2.

[22] “Electric VTOL Aircraft for Urban Air Mobility: Bauhaus Luftfahrt.” https://www.bauhaus-luftfahrt.net/en/research/systems-aircraft-technologies/electric-vtol-aircraft-for-urban-air-mobility/ (accessed Sep. 28, 2020).

[23] H. Zhang, L. Jia, L. Wang, and X. Xu, “Energy consumption optimization of train operation for railway systems: Algorithm development and real-world case study,” *J. Clean. Prod.*, vol. 214, pp. 1024–1037, Mar. 2019, doi: 10.1016/j.jclepro.2019.01.023.

[24] P. Salvador, P. Martínez, I. Villalba, and R. Insa, “Modelling energy consumption in diesel multiple units,” *Proc. Inst. Mech. Eng. Part F J. Rail Rapid Transit*, vol. 232, no. 5, pp. 1539–1548, May 2018, doi: 10.1177/0954409717737226.

[25] J. Wang and H. A. Rakha, “Electric train energy consumption modeling,” *Appl. Energy*, vol. 193, pp. 346–355, May 2017, doi: 10.1016/j.apenergy.2017.02.058.

[26] K.-K. Kee, B.-Y. Lau Simon, and K.-H. Yong Renco, “Prediction of Ship Fuel Consumption and Speed Curve by Using Statistical Method,” *J. Comput. Sci. Comput. Math.*, vol. 8, no. 2, pp. 19–24, Jun. 2018, doi: 10.20967/jcscm.2018.02.002.

[27] M. Jeon, Y. Noh, Y. Shin, O.-K. Lim, I. Lee, and D. Cho, “Prediction of ship fuel consumption by using an artificial neural network,” *J. Mech. Sci. Technol.*, vol. 32, no. 12, pp. 5785–5796, Dec. 2018, doi: 10.1007/s12206-018-1126-4.

[28] L. Yang, G. Chen, N. G. M. Rytter, J. Zhao, and D. Yang, “A genetic algorithm-based grey-box model for ship fuel consumption prediction towards sustainable shipping,” *Ann. Oper. Res.*, Mar. 2019, doi: 10.1007/s10479-019-03183-5.

[29] L. Guzzella and A. Sciarretta, *Vehicle Propulsion Systems*, Second Edi. Zürich: Springer, 2007.

[30] T. Grube, “Potentiale des Strommanagements zur Reduzierung des spezifischen Energiebedarfs von Pkw,” Berlin, Technische Universität, 2014.

[31] National Research Council of the National Academies, “Transitions to alternative vehicles and fuels,” 2013. doi: 10.17226/18264.

[32] R. Rajamani, *Vehicle dynamics and control*, First Edit., no. 12. Minnesota: Springer US, 2006.

[33] “Forward and Backward Euler Methods.” https://web.mit.edu/10.001/Web/Course_Notes/Differential_Equations_Notes/node3.html (accessed Sep. 16, 2020).

[34] T. J. Barlow, S. Latham, I. S. Mccrae, and P. G. Boulter, “A reference book of driving cycles for use in the measurement of road vehicle emissions,” Berkshire, 2009.

[35] “Emission Test Cycles: WLTC.” https://dieselnet.com/standards/cycles/wltp.php (accessed Jul. 10, 2020).

[36] F. Hülsmann, M. Mottschall, F. Hacker, and P. Kasten, “Konventionelle und alternative Fahrzeugtechnologien bei Pkw und schweren Nutzfahrzeugen – Potenziale zur Minderung des Energieverbrauchs bis 2050,” Freiburg, 2014. [Online]. Available: https://www.oeko.de/oekodoc/2105/2014-662-de.pdf.

[37] B. Cox, “Mobility and the Energy Transition: A Life Cycle Assessment of Swiss Passenger Transport Technologies including Developments until 2050,” 2018, [Online]. Available: https://doi.org/10.3929/ethz-b-000276298 Rights.

[38] F. Dünnebeil and H. Keller, “Monitoring emission savings from low rolling resistance tire labelling and phase-out schemes,” Heidelberg, 2015. [Online]. Available: http://transferproject.org/wp-content/uploads/2014/10/TRANSfer_MRV-Blueprint_lower-tires_EU.pdf.

[39] M. Wietschel *et al.*, “Klimabilanz , Kosten und Potenziale verschiedener Kraftstoffarten und Antriebssysteme für Pkw und Lkw,” Karlsruhe, 2019. [Online]. Available: https://www.isi.fraunhofer.de/content/dam/isi/dokumente/cce/2019/klimabilanz-kosten-potenziale-antriebe-pkw-lkw.pdf.

[40] R. Vijayagopal, D. N. Prada, and A. Rousseau, “Fuel Economy and Cost Estimates for Medium- and Heavy-Duty Trucks,” Illinois, 2019. [Online]. Available: http://www.osti.gov/.

[41] “Study on air traffic: Lufthansa dominates the skies over Germany.” https://ga.de/ga-english/news/lufthansa-dominates-the-skies-over-germany_aid-43675911 (accessed Sep. 13, 2020).

[42] “Germany: state of the market | Routesonline.” https://www.routesonline.com/news/29/breaking-news/283754/germany-state-of-the-market-/ (accessed Sep. 13, 2020).

[43] “1.A.3.a Aviation 2 LTO emissions calculator 2019 — European Environment Agency.” https://www.eea.europa.eu/publications/emep-eea-guidebook-2019/part-b-sectoral-guidance-chapters/1-energy/1-a-combustion/1-a-3-a-aviation-1-annex5-LTO/view (accessed Sep. 13, 2020).

[44] T. Kuminek, “Energy consumption in tram transport,” *Logist. Transp.*, vol. 18, no. 2, pp. 93–100, 2013.

[45] “GEMIS Database - IINAS.” http://iinas.org/database.html (accessed Sep. 30, 2020).

[46] Deutsche Bahn AG, “Deutsche Bahn 2018 Integrated Report On track towards a better railway,” Berlin, 2019. Accessed: Sep. 30, 2020. [Online]. Available: https://ib.deutschebahn.com/ib2018/fileadmin/PDF/IB18_e_web.pdf.

[47] T. Bründlinger *et al.*, “dena-Leitstudie Integrierte Energiewende. Impulse für die Gestaltung des Energiesystems bis 2050,” 2018. [Online]. Available: https://shop.dena.de/fileadmin/denashop/media/Downloads_Dateien/esd/9261_dena-Leitstudie_Integrierte_Energiewende_lang.pdf.

[48] “International Shipping – Analysis - IEA.” https://www.iea.org/reports/international-shipping (accessed Oct. 15, 2020).